Available online at www.sciencedirect.com
SCIENCE DIRECT®
PERGAMON
Renewable Energy 28 (2003) 1129–1142
RENEWABLE ENERGY
www.elsevier.com/locate/renene

Technical note

An on-line MPPT algorithm for rapidly changing illuminations of solar arrays

C. Hua [a,*], J. Lin [b]

[a] *Department of Electrical Engineering, National Yunlin University of Science and Technology, 123 University Road Section 3, Touliu City, Yunlin County, Taiwan, ROC*
[b] *Graduate School of Engineering Science and Technology, National Yunlin University of Science and Technologym, 123 University Road Section 3, Touliu City, Yunlin County, Taiwan, ROC*

Received 30 April 2002; accepted 2 October 2002

Abstract

Maximum power point tracking (MPPT) is usually used for a solar power system. Many maximum power tracking techniques have been considered in the past. The microprocessors with appropriate MPPT algorithms are favored because of their flexibility and compatibility with different solar arrays. Although the efficiency of MPPT algorithms is usually high, it drops noticeably in case of rapidly changing illumination conditions. The authors have proposed an improved MPPT algorithm based on the fact that the maximum power point (MPP) of solar arrays can be tracked accurately. The principle of energy conservation is used to develop the large- and small-signal model and transfer function for the solar power system. The work was carried out by both simulation and experiment on a current converter, by the digital signal processor (DSP) control, in MPPT mode under different illuminations. The results show that the proposed MPPT algorithm has successfully tracked the MPP in rapidly changing illumination conditions.

Keywords: Maximum power point tracking; Solar arrays; Digital signal processor; Principle of energy conservation

* Corresponding author. Tel.: +886-5-5342601-4250; fax: +886-5-5312042.
E-mail address: huacc@yuntech.edu.tw (C. Hua).

0960-1481/03/$ - see front matter © 2002 Elsevier Science Ltd. All rights reserved.
PII: S0960-1481(02)00214-8

1. Introduction

The maximum power points (MPPs) of solar array depend on insolation and temperature. It is most desirable that the operation of the load is close to the MPP of solar array. Since the MPP varies mainly with insolation, it is difficult to maintain optimal matching under various insolation levels. To deal with this problem, two methods are available to the system designer. The first method is direct-coupled method [1–4]; the solar array output power is delivered directly to the loads. In order to match the MPP of the solar array as close as possible, it is important to select the *I–V* characteristic of solar array by the *I–V* characteristics of load and/or vice versa. The second method is maximum power point tracking (MPPT) control, which continuously tracks and matches the output characteristics of the solar array to the input characteristics of the converter. Various methods of MPPT have been considered in the applications of solar arrays.

The incremental conductance (IncCond) method is often used in solar array systems [5] to track the MPPs by comparing the incremental and instantaneous conductance of the solar arrays. This method needs four sensors to perform the measurements for computations and decision-making. If the sensors or the system requires more conversion time, a large amount of power loss will result. The curve-fitting method [6,7] uses a numerical analysis method to find a linearly approximate relationship between the current of MPP and the photocurrent which is directly proportional to insolation. The method is only suitable for the location where the temperature variation is relatively small. The neural network-based MPPT has been proposed in Refs. [8,9]. After training the neural network with given data, the optimal operating point is identified, and the maximum power from the solar array will be estimated. Using this method, the data acquisition is more important than the MPPT algorithm. The perturbation and observation (P&Q) method, which moves the operating point toward the MPP by periodically increasing or decreasing the converter input voltage, is often used in many solar energy systems [10–13]. However, the P&Q method fails to quickly track the MPPs when there is a rapidly changing illumination of solar arrays. In this paper, an improved tracking algorithm is presented. Both simulation and experimental results demonstrate excellent performance under illumination variations.

The microprocessor is usually used to control the DC/DC converter for optimal operation which adds to the overall system cost considerably. In this paper, a solar array power system using a digital signal processor (DSP) is proposed. The MPPT is implemented in a software program with a self-tuning function, which automatically adjusts the array reference voltage and voltage step size to achieve the maximum power tracking under fast changing illumination conditions. By the controller using a DSP, real-time control maximum power tracking can be achieved rapidly and accurately by increasing the sampling frequency and improving the tracking algorithm. The proposed controller features MPPT, a battery charge regulation.

The state-space-averaging method [14] is widely used to derive expressions for small-signal characteristics of a pluse-width-modulated (PWM) converter. However, this method is sometimes tedious, especially when the converter equivalent circuit

contains a large number of elements. To obtain the models of DC/DC converters, the principle of energy conservation is used in this paper to derive the model and transfer function for the system [15]. The derived models are convenient for analyzing complicated converters, especially for those including parasitic components.

2. Solar array characteristics

Fig. 1 shows the simulated characteristic curves for the solar array at different insolations and different temperatures. From these curves, it is observed that the output characteristics of the solar array are nonlinear and vitally affected by solar radiation, temperature, and load conditions. Each curve has an MPP (P_{MAX}), which is the optimal operating point for the efficient use of the solar arrays. Fig. 2 illustrates the operating characteristic of the solar array under a given insolation. It consists of two regions: one is the current source region, and the other is the voltage source region. In the voltage source region, the internal impedance of the solar array is low on the right side of the power curve, and in the current source region, the internal impedance of the solar array is high on the left side of the power curve. The MPP of the solar array is located at the knee of the power curve. According to the maximum power transfer theory, the power delivered to the load is maximum when the source internal impedance matches the load impedance. Thus, the impedance

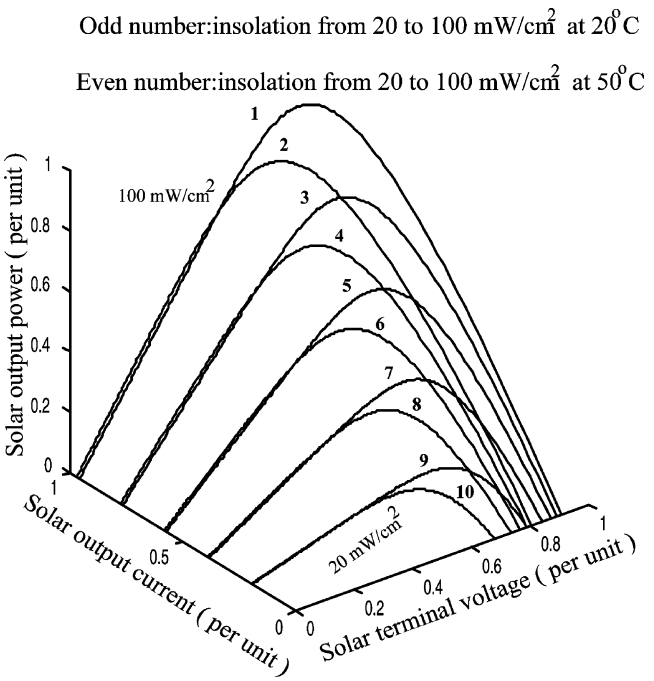

Fig. 1. Simulated solar array characteristic curves.

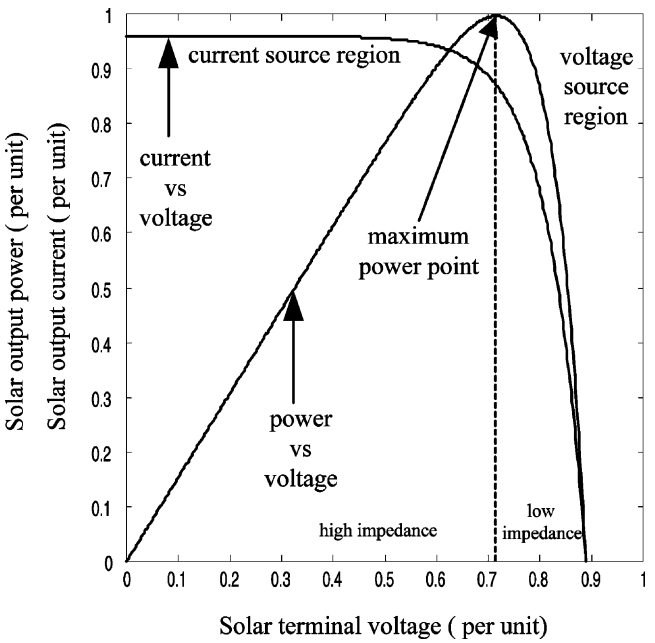

Fig. 2. Operating characteristic of a solar array.

seen from the current converter input side (can be adjusted by PWM control signal) needs to match the internal impedance of the solar array if the system is required to operate at or near the MPP of the solar array.

If the system operates on the voltage source region (namely low impedance) of solar array characteristic curve, the solar array terminal voltage will collapse. This behavior is due to the constant input power and the adjustable output voltage or output current of the converters. Therefore, the solar array is required to operate on the left side of the curve to perform the tracking process. In Ref. [16] the iterative algorithm is used in the tracking process. If the system tracks the MPP in the voltage source region, then the system will collapse because the algorithm ignores the negative impedance of the converter. A general approach [2] for the power feedback control is to measure and maximize the power at the load side. It is assumed that the solar array maximum power is equal to the maximum load power. However, this maximizes the power to the load, not the power from the solar array. A converter with MPPT offers high efficiency over a wide range of operating points; the full power may not be delivered to the load completely due to the power loss for a converter without MPPT. Therefore, the design of a high performance converter is a very important issue for a solar power system.

3. Propose tracking algorithm

The improved flowchart of maximum power tracking algorithm is shown in Fig. 3(a). The control algorithm starts the operation of a converter, which is initially at reset. The minimum allowable duty ratio is used to start a PWM controlled converter. With the MPPT control, the system will operate close to the MPPs of solar array. The flow chart consists of two loops: (1) insolation loop, and (2) temperature loop.

Insolation loop: When insolation changes from 100 to 40 mW/cm^2, the operating point changes from point 'a' to point 'b' as shown in Fig. 3(b). Point 'a' is the MPP of the solar array with insolation of 100 mW/cm^2, point 'c' is the MPP with insolation of 40 mW/cm^2, and point 'b' is on the right side of point 'c'. To avoid system collapse due to negative impedance characteristic, the reference voltage will continuously decrease until the operating point is close to a new MPP (point 'c'). On the contrary, if insolation changes from 40 to 100 mW/cm^2, then the reference voltage will continuously increase until the operating point is close to a new MPP (point 'a'). The power loss of the solar array can be reduced by using the proposed tracking method.

Temperature loop: The temperature loop starts to work when the insolation is approximately kept constant. Because of wind or other atmospheric conditions, the solar array temperature could be changed more significantly than the insolation. From the characteristic curves, the MPP of solar array will drift when the solar array temperature changes. In order to operate the solar array system in the maximum power tracking mode, the variation of solar array temperature has to be considered in the MPPT algorithm.

4. Model and control of the proposed system

4.1. System model

The state-space-averaging approach is widely used to derive expressions and analysis for small-signal characteristics of pulse-width-modulation (PWM) controlled DC/DC converters. It can predict the dynamic performance of the PWM converters. However, this approach has a drawback in that the computation process is very complicated when the converter equivalent circuit contains a large number of elements (including parasitic components). The principle of energy conservation is used in this paper to derive the circuit model and transfer function, which has the following advantages:

1. Switched resistors are replaced by the equivalent averaged resistors.
2. It can be used in the multi-switch circuits.
3. It can be easily applied in the circuit which consists of many non-switch elements.
4. The simulation and analysis of the circuit model is easy.

Fig. 4(a) shows the boost current converter and the equivalent circuit; the power

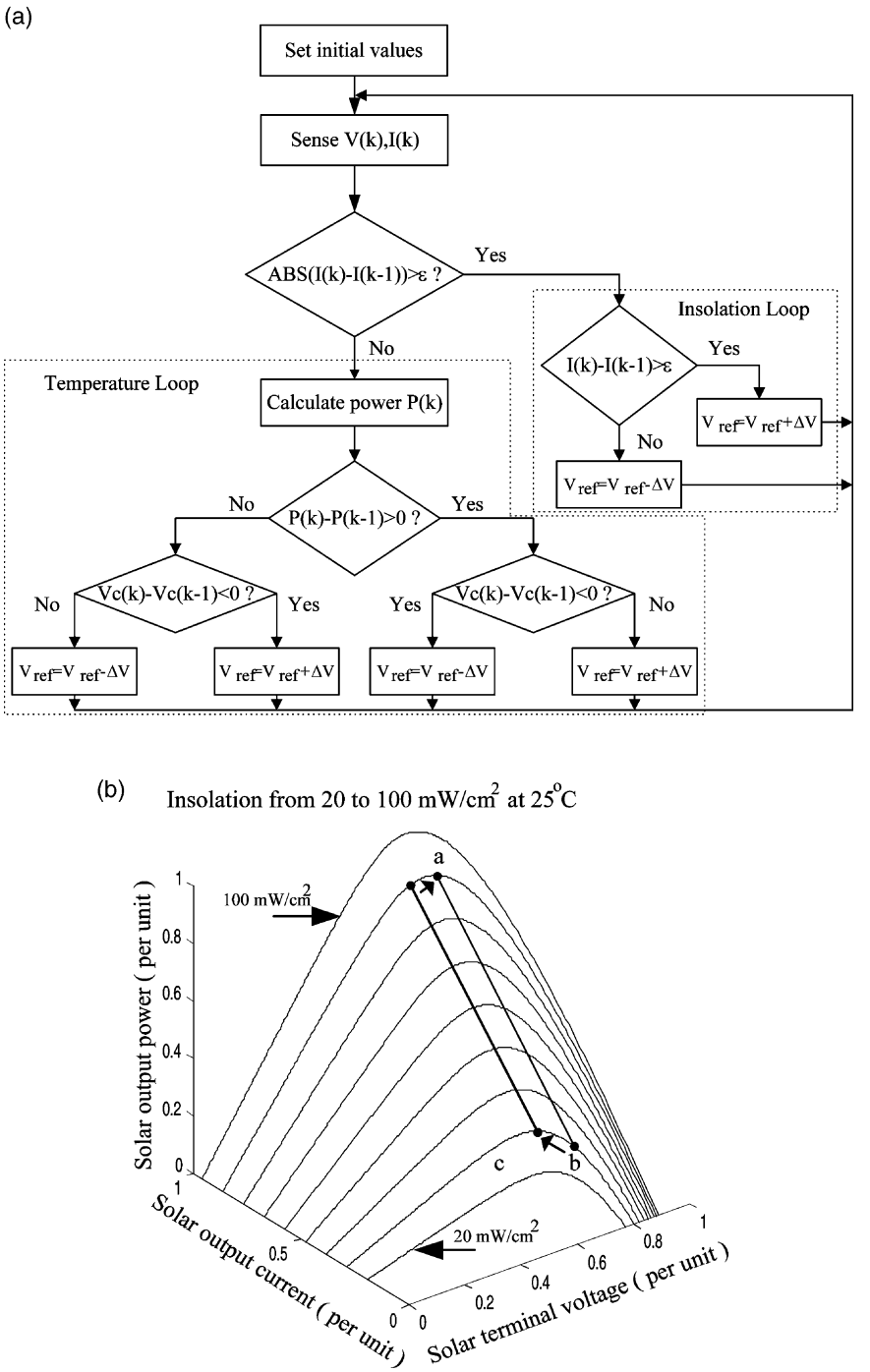

Fig. 3. (a) Flowchart of MPPT control. (b) MPP tracking process.

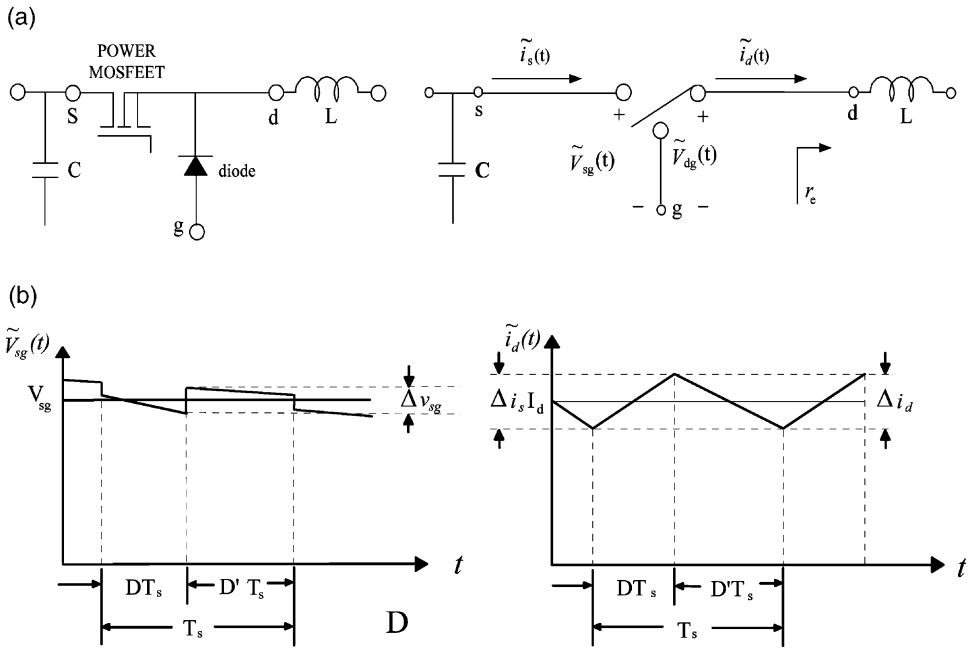

Fig. 4. (a) Boost current converter and equivalent circuit. (b) Waveforms for the terminal voltages and current.

MOSFET and diode can be combined into one network with three terminals s,d, and g, which represent active, passive, and common terminals, respectively. The three-terminal network is called the PWM-switch. Fig. 4(b) shows the waveforms for the terminal voltages and currents of the PWM-switch operating in the continuous conduction mode (CCM), where '~' denotes the instantaneous value of the variable.

Fig. 5(a) shows the system power circuit and the equivalent circuit model when it operates in CCM under PWM control. This model includes parasitic components and can be used for the analysis of the system under different modes. The r_{DS} is the resistance of the transistor, V_F is the threshold voltage of the diode, R_F is the forward resistance of the diode, r_L is the equivalent series resistance (ESR) of the inductor L, r_c is the equivalent series resistance (ESR) of the capacitor, R_{sh} is the equivalent

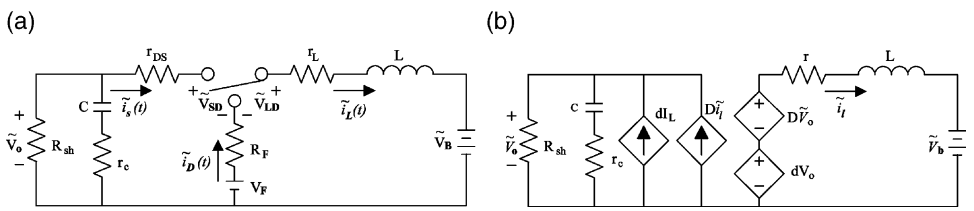

Fig. 5. (a) Equivalent circuit for PWM converter. (b) Small-signal model.

shunt resistor of the solar array. The small-signal model of the system can be obtained as shown in Fig. 5(b).

The equation of the inductor current, as shown in Fig. 5(b), is

$$\tilde{i}_{\mathrm{L}} = \begin{cases} \dfrac{\Delta i_{\mathrm{L}}}{DT_{\mathrm{S}}}t + I_{\mathrm{L}} - \dfrac{\Delta i_{\mathrm{L}}}{2} & 0 < t \leq DT_{\mathrm{S}} \\ -\dfrac{\Delta i_{\mathrm{L}}}{(1-D)T_{\mathrm{S}}}(t - DT_{\mathrm{S}}) + I_{\mathrm{L}} + \dfrac{\Delta i_{\mathrm{L}}}{2} & DT_{\mathrm{S}} < t \leq T_{\mathrm{S}} \end{cases} \tag{1}$$

4.1.1. Switch loss

The current into the switch is approximately $\tilde{i}_{\mathrm{L}}$ during the switch ON interval ($0 < t \leq DT_{\mathrm{S}}$), and the rms value of the switch current is

$$I_{\mathrm{S,rms}} = \sqrt{\frac{1}{T_S}\int_0^{DT_S} \tilde{i}_{\mathrm{S}}^2 \mathrm{d}t} = I_{\mathrm{S}}\sqrt{\frac{1+K^2}{D}} \tag{2}$$

where

$$K = \frac{V_{\mathrm{B}}(1-D)T}{\sqrt{12}I_{\mathrm{L}}L} \tag{3}$$

I_{S} is the average of $\tilde{i}_{\mathrm{S}}$, thus the loss of switch is

$$P_{\mathrm{S}} = I_{\mathrm{S}}^2 r_{\mathrm{DS}}\frac{1+K^2}{D} \tag{4}$$

4.1.2. Diode loss

The diode current is approximately $\tilde{i}_{\mathrm{L}}$ during the diode ON interval ($DT_{\mathrm{S}} < t \leq T_{\mathrm{S}}$), and the rms value of the diode current is

$$I_{\mathrm{D,rms}} = \sqrt{\frac{1}{T_S}\int_{DT_S}^{T_S} \tilde{i}_{\mathrm{D}}^2 \mathrm{d}t} = I_{\mathrm{D}}\sqrt{\frac{1+K^2}{1-D}} \tag{5}$$

where I_{D} is the average of $\tilde{i}_{\mathrm{D}}$, thus the loss of diode is

$$P_{\mathrm{D}} = I_{\mathrm{D}}^2 R_{\mathrm{F}}\frac{1+K^2}{1-D} \tag{6}$$

The power dissipated in the threshold voltage V_{F} is

$$P_{V_{\mathrm{F}}} = V_{\mathrm{F}} I_{\mathrm{D}} \tag{7}$$

4.1.3. Inductor loss

The rms value of the inductor current is

$$I_{L,rms} = I_L\sqrt{1 + K^2} \tag{8}$$

where I_L is the average of $\tilde{i}_L$, thus the loss of inductor is

$$P_L = r_L I_{L,rms}^2 = r_L(1 + K^2)I_L^2 \tag{9}$$

The reflection rule can be applied to move parasitic components from one branch to another, which results in another equivalent circuit model as shown in Fig. 8(c). In this figure, r is the equivalent averaged resistance and can be expressed as

$$r = [r_L + Dr_{DS} + (1-D)R_F](1 + K^2) \tag{10}$$

The disturbances of voltage, current and duty cycle can be expressed as the combination of the ac and dc components as shown in Fig. 5(b), and the nonlinear terms are neglected.

4.1.4. Transfer function

The charging voltage usually rises slowly, therefore, the voltage is assumed to be constant from the standpoint of the battery. The disturbance of the battery voltage is represented by a voltage perturbation $\tilde{V}_B$. The solar array is taken as a current source in this paper; thus, the solar array terminal voltage has to be adjusted to deliver the maximum power. The effect of a small perturbation of solar array terminal voltage on system stability has to be considered carefully. The small-signal model of the control-to-output transfer function is expressed as

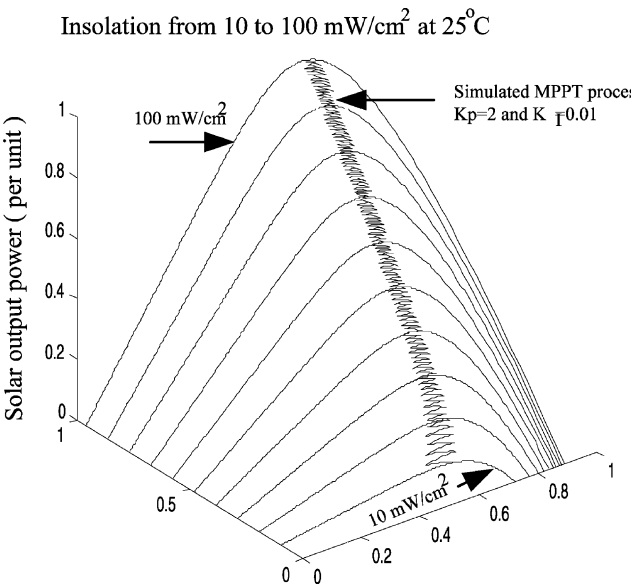

Fig. 8. Simulated MPPT process with the PI compensator.

$$T_P(S) = \left.\frac{\tilde{V}_O(S)}{d(S)}\right|_{\tilde{V}_b=0} \tag{11}$$

From the circuit in Fig. 5(d),

$$v_o = -(Di_l + dI_L)\frac{R_{sh} \times (r_c cs + 1)}{R_{sh} cs + r_c cs + 1} \tag{12}$$

$$i_l = \frac{Dv_o + dV_O}{r + sL} \tag{13}$$

Substitution of Eq. (13) into Eq. (12), and rearranging yields

$$T_P(S) = \left.\frac{\tilde{V}_O(S)}{d(S)}\right|_{\tilde{V}_b=0} = \frac{V_o r_c \quad (S + \omega_c)(S + \omega_l)}{D(R_{sh} + r_c)S^2 + 2\xi_t \omega_t S + \omega_t^2} \tag{14}$$

where

$$\omega_c = \frac{1}{r_c c} \tag{15}$$

$$\omega_l = -\frac{1}{L}(D^2 R_{sh} - r) \tag{16}$$

$$\omega_t = \sqrt{\frac{r + R_{sh} D^2}{2C(R_{sh} + r_c)}} \tag{17}$$

$$\xi_t = \frac{[r(R_{sh} + r_c) + R_{sh} r_c D^2]C + L}{2\sqrt{LC(R_{sh} + r_c)(r + R_{sh} D^2)}} \tag{18}$$

4.2. System control

Fig. 6 shows the power circuit of the proposed control. The system consists of a nonlinear current source, a DC/DC current converter, a battery set, and a digital control circuit based on a DSP. System control consists of two loops: the MPPT loop is used to set a corresponding V_{ref} to the charger input, and the voltage loop is used to regulate the solar array output voltage according to the V_{ref}, which is set in the MPPT loop. The functions in the two loops are performed by a DSP. The DSP senses the solar array current and voltage, calculates the solar array output power, power slope and V_{ref} to track the MPP. The control algorithm can be expressed as the following equation:

$$V_{ref}(k + 1) = V_{ref}(k) \pm \Delta V \tag{19}$$

The ΔV is the amount of disturbance, which is self-tuning depending on the power difference, and the sign of ΔV is determined by the power slope.

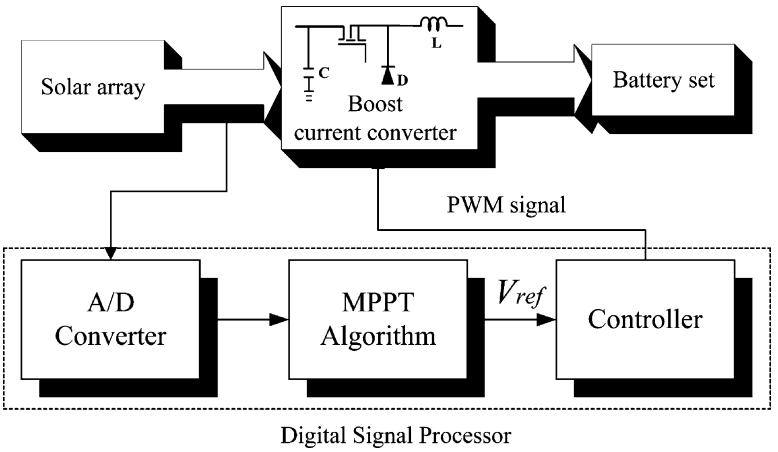

Fig. 6. Solar array power system circuit.

5. Simulations and experimental results

The proposed solar array system was implemented using a digital controller based on the Texas TMS320C240 DSP, as shown in Fig. 6. The system consists of a nonlinear current source as the power source, a DC/DC current converter power stage as the power processing unit, a battery set as the load, and a DSP as the controller. The National Instruments Company AT-MIO-16E-10 is used as the data acquisition board with Libview software drive for interfacing.

The prototype solar array maximum power tracking converter and the DSP controller were built and tested. Sixteen modules of solar array (Solarex MSX60) in a series are used in the system. Each module has a maximum power output of 60 W. The control software was written in DSP language and was tested and debugged using the TMS320 simulator running on the host PC. Finally, the software was downloaded to the DSP board.

The system is unstable without a PI compensator, as shown in Fig. 7(a), and its phase margin, PM = −18.54, is very poor. With a PI compensator in Fig. 7(c), the system performance is improved; the phase margin of Bode diagram is better as shown in Fig. 7(b). Fig. 8 shows the simulated result of the system with the PI compensator, while the insolation is changing linearly and the temperature is set at 25 °C. The MPPT process moves along a zig-zag path close to the MPPs of the solar array.

Fig. 9 shows the experimental result of the MPPT for the solar array system at 50 °C and insolation variation of 20–70 mW/cm^2. From the above figures, the fast changes in solar array output power and output voltage are observed, and the solar array output power is able to follow the fast atmospheric variations step-by-step. It is shown that increasing the execution speed of the P&O method enables the system to follow the fast changes of the insolation and achieve the maximum power transfer from the solar array. The ratios of experimental voltage/power to theoretical

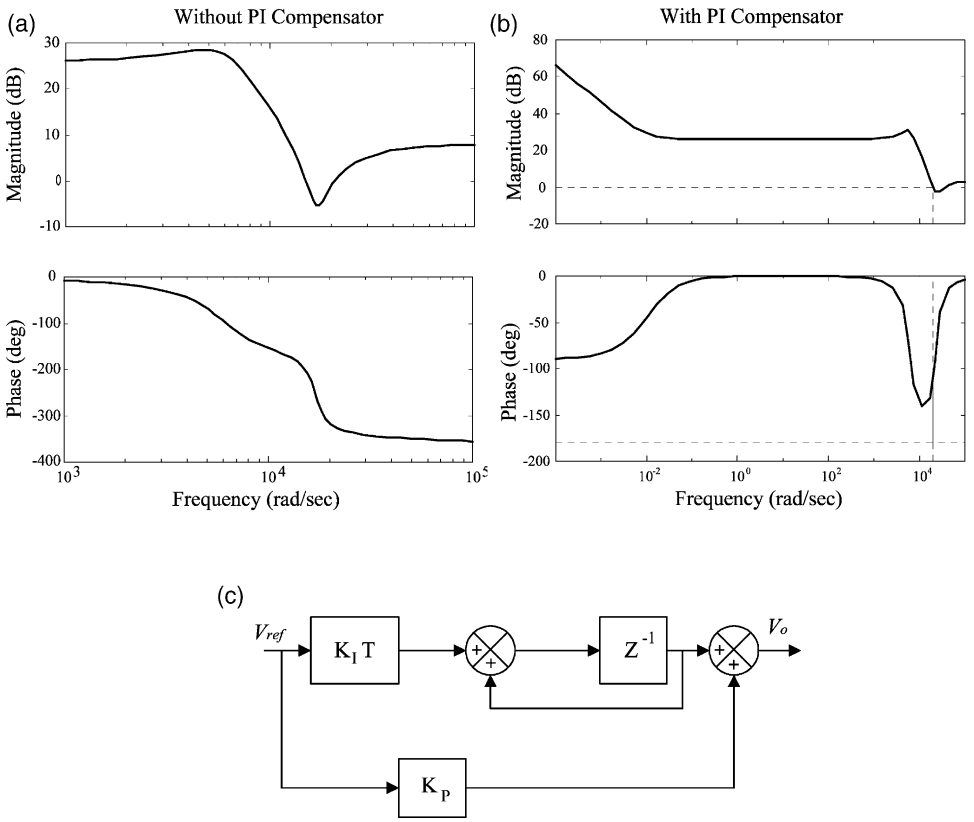

Fig. 7. Control-to-output Bode diagram. (a) Without PI compensator. (b) With PI compensator. (c) Digital PI compensator.

voltage/power, as shown in Fig. 9(c) and (d), range from 0.98 to 1.02. Therefore, the proposed MPPT algorithm shows good performance for the solar array system.

6. Conclusions

The purpose of maximum power tracking is to transfer the maximum possible power to the load from the solar array. The principle of energy conservation has been used to analyze the boost current converter and to derive the large-signal, small-signal model and transfer function for the system. The proposed MPPT algorithm, which uses the power as the control variable based on the perturbation and observation method, only requires two sensors.

The system has a good response under fast changing atmospheric conditions, and a better performance can be obtained by increasing the execution speed and simplifying the tracking algorithm. A DSP-based controller is used to implement the proposed MPPT and control algorithm; simulated and experimental results are presented to

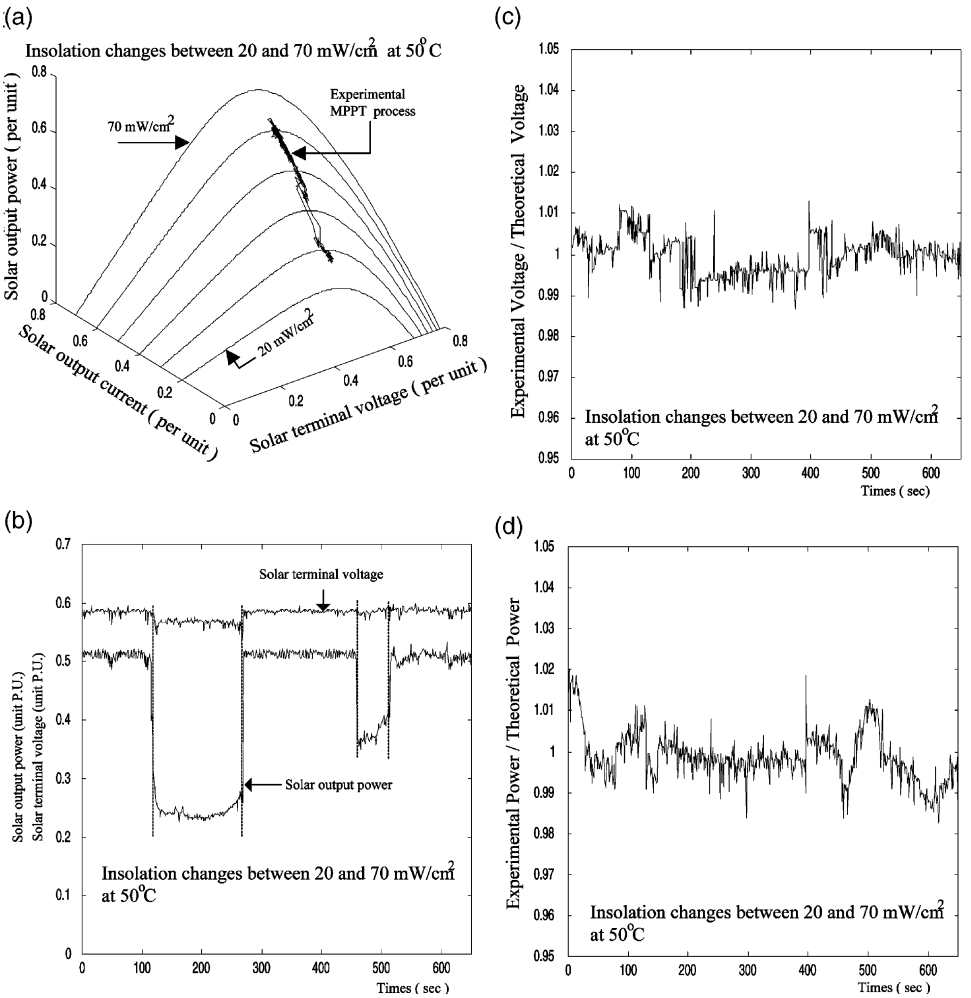

Fig. 9. Experimental result for insolation change between 20 and 70 mW/cm^2. (a) Tracking process. (b) Solar array output power and voltage. (c) Ratio of experimental power to theoretical power. (d) Ratio of experimental voltage to theoretical voltage.

verify the system performance. Because the insolation is usually proportional to the business power, the incorporation of the proposed solar power system with other power equipment can be used in the applications of active power filters, uninterruptible power supplies, distributed power systems, etc.

Acknowledgements

This research is sponsored by National Science Council under the contract NSC 89-TPC-7-224-052.

References

[1] Applebaum J. The quality of load in a direct-coupling photovoltaic system. IEEE Trans Energy Conver 1987;2(4):534–41.
[2] Khouzam KY. Optimum load matching in direct-coupled photovoltaic power systems—application to resistive loads. IEEE Trans Energy Conver 1990;5(2):265–71.
[3] Schoeman JJ, Van Wyk JD. A simplified maximum power controller for terrestrial photovoltaic panel arrays. In: IEEE Power Electronics Specialists Conference. 1982. p. 361–7.
[4] Fan WZ, Balachander MK. Dynamic performance of a DC shunt motor connected to a photovoltaic array. IEEE Trans Energy Conver 1988;3(3):613–7.
[5] Wasynczuck O. Dynamic behavior of a class of photovoltaic power system. IEEE Trans Power Ap Syst 1983;102(9):3031–7.
[6] Alghuwainem SM. Matching of a DC motor to a photovoltais generator using a step-up converter with a current-locked loop. IEEE Trans Energy Conver 1994;9(1):192–8.
[7] Chiang SJ, Chang KT, Yen CY. Residential photovoltaic energy storage system. IEEE Trans Ind Electron 1998;45(3):385–94.
[8] Hiyama T, Kouzuma S, Imakubo T. Identification of optimal operating point of PV modules using neural network for real time maximum power tracking control. IEEE Trans Energy Conver 1995;10(2):360–7.
[9] Hiyama T, Kitabayashi K. Neural network based estimation of maximum power generation from module using environmental information. IEEE Trans Energy Conver 1997;12(3):241–7.
[10] Bose BK, Szczesny PM, Steigerwald RL. Microcomputer control of a residential photovolatic power conditioning system. IEEE Trans Ind Appl 1985;21(5):1182–91.
[11] Huynh P, Cho BH. Design and analysis of microprocessor controlled peak power tracking system. In: Proceedings of the 27th IECEC, vol. 1. 1992. p. 67–72.
[12] Yongji H, Deheng L. A new method for optimal output of a solar cell array. In: Proceeding of the IEEE International Symposium on Industrial Electronics, vol. 1. 1992. p. 456–9.
[13] Salameh Z, Dagher F, Lynch WA. Step-down maximum power point tracker for photovoltaic system. Sol Energy 1991;46(5):279–82.
[14] Middlebrook RD, Cuk SA. General unified approach to modeling switching-converter power stages. In: IEEE Power Electronics Specialists Conference. 1976. p. 18–34.
[15] Czarkowski D, Kazimierczku NK. Static- and dynamic circuit model of PWM buck derived DC-DC Converters. IEE Proc-G 1992;139(6):669–79.
[16] Altas IH, Sharaf AM. A novel on-line MPP search algorithm for PV arrays. IEEE Trans Energy Conver 1996;11(4):748–54.